Document downloaded from:

http://hdl.handle.net/10251/157305

This paper must be cited as:

Challita, F.; Rodrigo Peñarrocha, VM.; Rubio Arjona, L.; Reig, J.; Juan-Llácer, L.; Pascual-García, J.; Molina-García-Pardo, J.... (2019). On the Contribution of Dense Multipath Components in an Intrawagon Environment for 5G mmW Massive MIMO Channels. IEEE Antennas and Wireless Propagation Letters. 18(12):2483-2487. https://doi.org/10.1109/LAWP.2019.2940831

The final publication is available at

https://doi.org/10.1109/LAWP.2019.2940831

Copyright Institute of Electrical and Electronics Engineers

Additional Information

© 2019 IEEE. Personal use of this material is permitted. Permissíon from IEEE must be obtained for all other uses, in any current or future media, including reprinting/republishing this material for advertisíng or promotional purposes, creating new collective works, for resale or redistribution to servers or lists, or reuse of any copyrighted component of this work in other works.

On the contribution of Dense Multipath Components in an intra-wagon environment for 5G mmW Massive MIMO channels

Frédéric Challita[1], Vicent M. Rodrigo-Peñarrocha[2], Lorenzo Rubio[2], Juan Reig[2], Leandro Juan-Llácer[3], Juan Pascual-García[3], José-María Molina-García-Pardo[3], Martine Liénard[1], Davy P. Gaillot[1]

***Abstract*—In this letter, the dependence of the specular (SMC) and dense multipath components (DMC) to the inter-user spatial correlation and sum-rate capacity of a massive multi-user MIMO (MU-MIMO) setup is evaluated from measurements conducted inside an underground subway wagon at the 25 - 40 GHz candidate frequency bands for 5G systems. The radio channel consists in a 7 $\times$ 7 uniform rectangular array (URA) acting as access point (AP) for 8 users uniformly distributed in the wagon. The DMC power ratio is observed to be distance- and frequency-dependent as the SMC and DMC exhibit different propagation mechanisms. Remarkably, it is reported that the inter-user spatial correlation computed with DMC offers the best favorable propagation for a massive MIMO setup whereas SMC contribute to the users correlation. Hence, correlation is found to be strongly dependent on the DMC ratio frequency characteristics. In addition, better inter-user correlation and sum-rate capacity values are obtained as the frequency is increased. These results highlight the need to include DMC in 5G massive MIMO channel models and emulators to improve their accuracy at the system level.**

***Index Terms*—Massive MIMO, Multiuser channels, Spatial Correlation, DMC.**

I. Introduction

Massive MIMO is a cutting edge and emerging technology capable of filling the gap for many 5G requirements [1] in the race to tackle the ever-increasing demand for multiple use-cases [2]. The increasing number of elements can alleviate the effect of small scale fading and reduce inter-user interference using spatial division to simultaneously form separate beams [3]. Linear precoding schemes can be applied [4] and become nearly optimal when the Tx-Rx ratio becomes large [5]. An overview of massive MIMO can be found in [6].

Manuscript received May 6, 2018; accepted June 14, 2018.

This work was funded by MINECO, Spain, under the national projects TEC2016-78028-C3-2-P and TEC2017-86779-C2-2-R and supported through the ELSAT2020 OS4 SMARTIES program co-financed by the European Union with the European Regional Development Fund, the French state and the Hauts de France Region Council.

F. Challita, D. P. Gaillot, and M. Liénard are with the University of Lille, IEMN, Bâtiment P3,Villeneuve d'Ascq, 59655 FR e-mail: frederic.challita@univ-lille.fr.

V M. Rodrigo-Peñarrocha, L. Rubio and J. Reig are with the iTEAM Research Institute, Universitat Politècnica de València, 46022 Valencia, Spain email:{ vrodrigo; lrubio; jreigp}@dcom.upv.es.

J-M. Molina-García-Pardo, Leandro Juan-Llácer and Juan Pascual-García are with the Dpto. Tecnologías de la Información y las Comunicaciones, Universidad Politécnica de Cartagena, Cartagena, Spain e-mail: josemaria.molina@upct.es

A good understanding of the massive MIMO radio channel and its underlying propagation and inter-user correlation mechanisms are necessary for wireless systems design. Specular multipath components (SMC) are generally well accounted for in channel models, but are not the only contributors. Dense multipath components (DMC) which includes diffuse scattering and weak SMC, are now widely recognized as a significant radio channel component in indoor scenarios [7] and first reported in [8] from MIMO channel measurements. It can be modeled from the channel impulse response as a decaying exponential residual power delay profile (PDP) after the SMC is removed. It is generally acknowledged that the contribution of DMC to the total radio channel received power (DMC power ratio) is large at sub-6 GHz band for indoor scenarios [8], [9] and decreases as the frequency is increased [10]. Polarimetric MIMO measurements at 1.3 GHz in a large industrial hall [11] and at 5.3 GHz [12] reported DMC power ratio values varying between 10% and 95% depending the presence of line-of-sight (LOS) conditions and Tx-Rx distance. Larger ratios were observed at 60 GHz for closed environments [13] compared to more open environments [14] at 60 and 70 GHz. Significant influence of DMC at 11 GHz on the structure of the MIMO channel was also discussed in [15]. Hence, several works conclude on including diffuse scattering in radio channel models and tracing tools to increase the accuracy even at millimeter-wave (mmW) frequencies [16]. However, few studies can be found in the literature for massive MIMO radio channels but, nonetheless, indicate that DMC and SMC are comparable. Indoor measurements for DMC contribution are reported at 6 GHz in obstructed line-of-sight (OLOS) and LOS conditions [17] and the variance of DMC parameters across the large-scale array at 11 GHz are analyzed and modeled in [18]. Despite its recognized contribution to the radio channel, it can be safely concluded that the influence of DMC on different aspects of a massive MIMO system, especially correlation at Rx side, has not been investigated to date. Only in [19], the spatial receiver decorrelation was linked to overall phase variation across a massive URA for an indoor scenario at 94 GHz. Moreover, different 5G mmW bands should be agreed at WRC-19, under Agenda Item 1.13, for instance, 24.25-29.5, 31.8-33.4, 37-43.5, and 45.5-50.2 GHz. To this purpose, channel measurements in these frequency bands are needed. In [20], at least five future railway service scenarios are defined for 5G, including intra-wagon, but analysis of the massive MIMO characteristics and potential

for these scenarios is missing. The contributions of this letter are the following:

1) Experimentally investigating an intra-wagon environment at 4 potential 5G frequency bands. The frequency characteristics of SMC, DMC, extracted using the RiMAX estimator, are investigated for all bands in the same setup.
2) Evaluating the contribution of the estimated SMC, DMC parameters to the receiver spatial correlation by separately considering the decorrelation due to each mechanism at each frequency band. This evaluation is also linked to the DMC power ratio and its influence on spatial separation between users. To the authors' best knowledge, this analysis is done for the first time with massive MIMO channel measurements. The origins of the frequency-dependence mechanisms of the inter-user correlation are identified which is insightful for 5G mmW indoor channel models.
3) System performance using zero-forcing precoding and equal power allocation is also applied to link spatial degrees of freedom of the channel (affected by DMC power ratio) to eventual provided performance improvements using sum-rate capacity analysis.

II. Channel Measurement

A. Environment

The measurement campaign took place in an underground convoy owned by the public railway company FGV (Ferrocarriles de la Generalitat Valenciana) in Valencia, Spain. The convoy consists in four connected wagons forming a single space and the total interior dimensions are 55.25 $\times$ 2.55 $\times$ 2.15 m (L $\times$ l $\times$ H) [21]. The space is furnished with resin modeled glass fiber reinforced side seats, stainless steel handholds (same material for the roof). The floor is made of stratified rubber, the windows of laminated glass and the doors are of glass and aluminum. The environment can be characterized as rich-multipath due to the presence of numerous metallic elements in the structure. An interior view of the wagon with one Tx-Rx position is illustrated in Fig. 1(a).

B. Measurement Setup

Channel transfer functions (CTF) are measured in the frequency domain using a vector network analyzer (VNA) that extracts the frequency-dependant transmission coefficient $s_{21}(f)$. The system has been through calibrated so that the measured CTF takes into account the joint response of the channel and the Tx-Rx antennas. Identical vertical polarized ultra-wideband antennas with omni-directional pattern in azimuth were used at the access point (AP) and user positions. Radio over fiber (RoF) was added between the transmitter and the VNA to avoid high losses at mmW frequencies and increase the dynamic range. The massive AP array was a 7×7 planar uniform rectangular array (URA) constructed with a positioning system (3.04 mm element-spacing) controlled by a personal computer. As shown in Fig. 1(b), 8 users are considered for the AP with Tx-Rx distance between 5 and 50 m. Using channel reciprocity, the AP can be considered as the massive MIMO transmitter serving 8 receiver positions acting as users. The CTF were measured from 25 to 40 GHz with a 15 GHz span (32.5 GHz central frequency) in order to analyze and compare the propagation conditions for the potential frequency bands proposed by the WRC. The four studied bands and other system parameters are presented in Table I. The intermediate frequency (IF) filter at the VNA of 100 Hz was chosen as a compromise between acquisition time and dynamic range. For each $s_{21}(f)$, an average of two traces was performed by the VNA to reduce thermal noise. The acquisition time for each position was about 2 hours during which doors of the convoy remained closed guaranteeing stationarity. The measurements were collected under LOS conditions at all times.

TABLE I
Sounding parameters, AP array characteristics and studied bands

VNA	Center Frequency	32.5 GHz
	Span Bandwidth	15 GHz
	Number of frequency points M_f	8192
	Frequency Resolution	1.83 MHz
	Tx Power	-17 dBm
Bands	B1	25 - 27.5 GHz
	B2	27.5 - 29.5 GHz
	B3	31.8 - 33.4 GHz
	B4	37 - 40 GHz

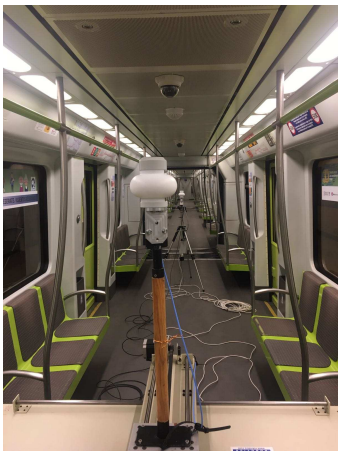

(a)

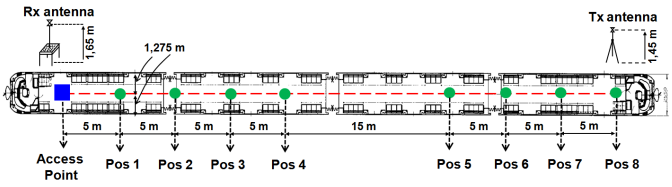

(b)

Fig. 1. (a) Interior view of the convoy with the AP and one user position and (b) schematic of the setup.

III. Evaluation Metrics

A. SMC and DMC Estimation

The sampled array response for user position k and AP antenna m, $\mathbf{h}_{km} \in \mathcal{C}^{1\times M_f}$, can be written as the sum of SMC contribution $\mathbf{s}_{km}$ and DMC contribution $\mathbf{d}_{km}$. It is common to

consider that $\mathbf{h}_{km}$ follows a multivariate circularly symmetric complex Gaussian distribution [8].

$$\mathbf{h}_{km} = \mathbf{s}_{km}(\theta_s) + \mathbf{d}_{km}(\theta_d). \quad (1)$$

θ_s regroups the SMC geometrical parameters (angle of departure in azimuth and elevation $\theta_{az\backslash el}$, time delay τ, and complex amplitudes) whereas θ_d determines the DMC process and related covariance matrix. The high-resolution parametric estimator RiMAX has been used to estimate θ_s and θ_d from the measured radio channels using a deterministic and stochastic maximum likelihood approach, respectively [8]. The DMC PDP $\psi(\tau)$ can be described by an exponential decay characterized by a reverberation time derived from room electromagnetics theory [22]. The reverberation ratio or DMC power ratio R defined as the contribution of DMC to the radio channel for a given user position is given by:

$$R = \frac{P_{\text{DMC}}}{P_{\text{DMC}} + P_{\text{SMC}}}, \quad (2)$$

with P the received power at one user position, averaged over all AP array antennas and frequency points of the considered band.

B. Rx spatial correlation

Benefits of massive MIMO systems arise from users orthogonality and subsequent capacity improvements due to the spatial degrees of freedoms offered by the radio channel. For a multi-user (MU) scenario, the orthogonality can be assessed with the Rx spatial correlation ρ_{Rx} [19]. The receiving correlation matrix $\mathbf{R}_{\text{Rx}}$ can be expressed as:

$$\mathbf{R}_{\text{Rx}} = \mathbf{E}\{\mathbf{H}\mathbf{H}^H\}, \quad (3)$$

and then normalized with the corresponding variances of the channel vectors. ρ_{Rx} is derived from $\mathbf{R}_{\text{Rx}}$ by averaging the off-diagonal upper triangular part of $\mathbf{R}_{\text{Rx}}$ owing to its Hermitian symmetry.

C. Sum-rate capacity

One prospect of massive MIMO systems is the relationship between receiver spatial correlation and sum-rate capacity. The capacity of a system (in bits/s/Hz) depends on many factors : signal to interference-plus-noise ratio (SINR), power allocation, precoding schemes, etc. Under perfect channel knowledge hypothesis, the achievable ergodic rate is a logarithmic function of the SINR:

$$C = \sum_{i=1}^{K} \log_2(1 + \text{SINR}_k), \quad (4)$$

where the SINR_k can be found as :

$$\text{SINR}_k = \frac{p_k |\mathbf{h}_k \mathbf{w}_k|^2}{\sum_{i=1,\ i\neq k}^{K} p_i |\mathbf{h}_k \mathbf{w}_i|^2 + \sigma_n^2}, \quad (5)$$

and p_k designates power allocated to the k^{th} user and $\mathbf{w}_k$ the precoding vector. In this work, the zero-forcing (ZF) precoder is considered with equal power allocation. If a maximum-ratio transmitter (MRT) was used instead, the 8 LOS positions would suffer from additional interference and lower performance compared to ZF.

IV. Results

a) PDP: As an example, the measured PDP and estimated DMC PDP (averaged over all AP array antennas) are illustrated in Fig. 2 for positions 1 and 8 in the 37-40 GHz band (B4). It is observed that the measured PDP and estimated DMC differ greatly between the two positions highlighting the distance-dependence of those mechanisms. Moreover, the reverberation time for position 8 is larger (longer decay). This result is in contrast with reported results for indoor scenarios wherein the reverberation time was found nearly constant for any user positions in the environment [11].

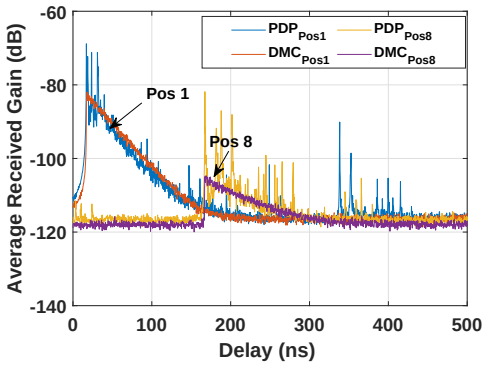

Fig. 2. Measured and estimated DMC PDP for positions 1 and 8 in the 37-40 GHz band.

b) DMC power ratio: The difference between the SMC and DMC propagation mechanisms are further illustrated in Fig. 3 which presents the evolution of the estimated SMC gain (a), estimated DMC gain (b) and DMC power ratio (c) as a function of distance and frequency band. First, the results indicate that the SMC gain is much more sensitive to frequency compared to DMC. It appears B1 is the most favorable band for propagation and B4 the least. Moreover, SMC and DMC gain both increase once a Tx-Rx distance of 40 m is reached. In addition, the decay mechanisms between SMC and DMC differ as shown in Fig. 3(c). Overall, the DMC ratio decreases with distance but increases with frequency for this scenario ($\sim$35% average for B4 and $\sim$ 18 % for B2). Finally, maximum R values are obtained at 25 m up to 40% and 50% for B3 and B4, respectively, showing that the DMC can take a large part of the total radio channel power in this scenario. This bell behavior was also reported in [23], [24] and is due to the different decaying mechanisms of the SMC and DMC.

c) Spatial Channel Correlation: Figure 4 presents the evolution of ρ_{Rx} with the number of AP elements for the estimated SMC, DMC as well as the measured channel $\mathbf{H}$ and the independent and identically distributed (i.i.d.) Rayleigh case. The reconstructed channel (from DMC and SMC estimates as in Eq. 1) was found to give similar results compared to the measured channel, thus only the measured channel was represented. This approach quantitatively provides insight into the origins of the inter-user correlation mechanisms.

As expected in massive MIMO setups, the results clearly show, for all considered mechanisms, that a better inter-user decorrelation is achieved when the number of active AP antennas is increased. Nonetheless, some notable conclusions

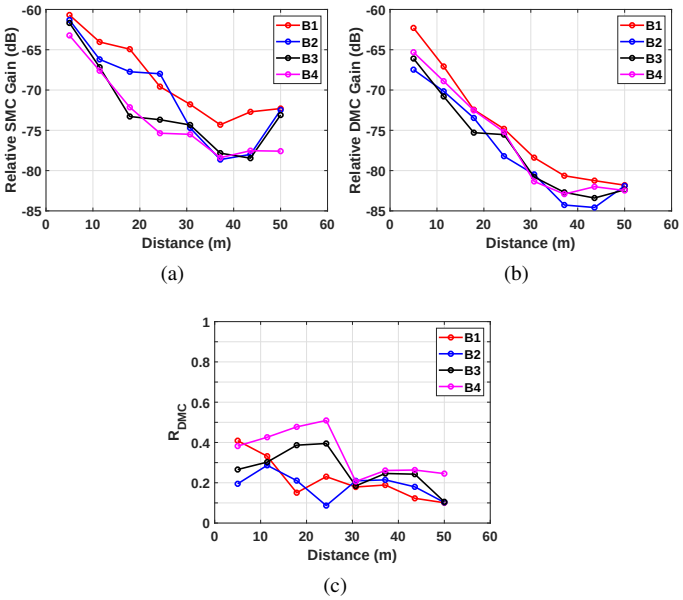

Fig. 3. Evolution of the received gain with distance for (a) SMC, (b) DMC, and (c) DMC power ratio.

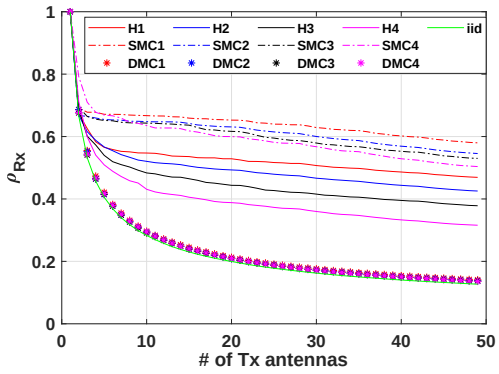

Fig. 4. Dependence of ρ_{Rx} on the number of AP array antennas for the estimated SMC, DMC, H, and i.i.d. for all frequency bands.

can be drawn. ρ_{Rx} obtained from the measured radio channels is frequency-dependent and decreases as the frequency is increased. A deeper analysis reveals that ρ_{Rx} computed for DMC is the same than for the ideal i.i.d. case and is, therefore, not frequency-dependent which is rather unexpected. ρ_{Rx} computed for SMC depends on frequency and decreases as the frequency is increased. Hence, the end part of the considered mmW spectrum slightly favors the SMC inter-user correlation. Overall, it can be concluded that DMC is the sole contributor of the decorrelation mechanisms between users whereas SMC introduces correlation at Rx side. Evidently, the measured channel correlation is between both curves with values depending upon the DMC power ratio distribution. Indeed, since DMC ratio values below 0.5 are obtained in this scenario, ρ_{Rx} is closer to the SMC correlation curve rather than the DMC one. B4 presents the lowest correlation values whereas B1 presents the largest values for the overall channel and SMC. This is due to the fact that the DMC ratio is the largest on average for B4 and the lowest for B1. In conclusion, the correlation mechanisms strongly depend on the DMC contribution in the channel. Consequently, in highly diffuse environments for which DMC dominates, ρ_{Rx} would converge to the i.i.d. case even if the receivers are in strong LOS conditions like the presented scenario.

d) Sum-rate Capacity: Finally, Fig. 5 presents the sum-rate capacity computed with a 15 dB SNR and ρ_{Rx} for the four considered frequency bands as a function of active AP antennas. The number of antennas was varied from to 9 to 49 because of the ZF precoding since 8 users are considered. It can be observed that these two parameters are highly correlated and the larger the sum-rate capacity the lowest ρ_{Rx}. Hence, spectral efficiency performance is degraded when ρ_{Rx} values are large. In addition, the sum-rate capacity increases with frequency such that the largest values are obtained for B4 for which ρ_{Rx} is the lowest. Clearly, since ρ_{Rx} strongly depends on the DMC contribution to the radio channel (Fig. 4), it is concluded that this propagation mechanism favors larger sum-rate capacity values.

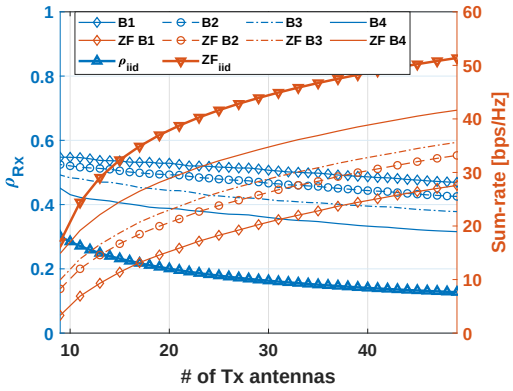

Fig. 5. Evolution of the sum-rate capacity with M for all frequency bands and SNR = 15 dB.

V. Conclusion

In this work, 49 × 8 massive MIMO measurements in an indoor subway intra-wagon environment are presented for four potential 5G frequency bands. The frequency-dependence characteristics of the SMC and DMC estimated with RiMAX are highlighted. The DMC power ratio increases with frequency but decreases with distance. However, the SMC and DMC contribution to the inter-user correlation strongly differ. For instance, DMC and the massive MIMO i.i.d. canonical model provide similar inter-user correlation for all frequency bands. In contrast, the correlation computed for SMC is large and presents a small dependence to frequency. Consequently, the measured correlation is found to depend upon the DMC ratio more than the frequency-dependence of the SMC. For the considered scenario, it can be concluded that the diffuse nature of the radio channels favors decorrelating the users and sum-rate capacity as the frequency is increased. Hence, DMC should not be overlooked when designing 5G radio channel models to evaluate the performance of massive MIMO systems. Future works include a deeper investigation of the overall performance as a function of the DMC characteristics for different power allocation and precoding schemes.

REFERENCES

[1] A. Gupta and R. K. Jha, "A Survey of 5G Network: Architecture and Emerging Technologies," *IEEE Access*, vol. 3, pp. 1206–1232, 2015.

[2] A. Osseiran, F. Boccardi, V. Braun, K. Kusume, P. Marsch, M. Maternia, O. Queseth, M. Schellmann, H. Schotten, H. Taoka, H. Tullberg, M. A. Uusitalo, B. Timus, and M. Fallgren, "Scenarios for 5G mobile and wireless communications: the vision of the METIS project," *IEEE Communications Magazine*, vol. 52, no. 5, pp. 26–35, May 2014.

[3] T. L. Marzetta, "Noncooperative Cellular Wireless with Unlimited Numbers of Base Station Antennas," *IEEE Transactions on Wireless Communications*, vol. 9, no. 11, pp. 3590–3600, November 2010.

[4] X. Gao, O. Edfors, F. Rusek, and F. Tufvesson, "Linear Pre-Coding Performance in Measured Very-Large MIMO Channels," in *Vehicular Technology Conference (VTC Fall), 2011 IEEE*, Sept 2011, pp. 1–5.

[5] E. Björnson, M. Bengtsson, and B. Ottersten, "Optimal Multiuser Transmit Beamforming: A Difficult Problem with a Simple Solution Structure ," *IEEE Signal Processing Magazine*, vol. 31, no. 4, pp. 142–148, July 2014.

[6] L. Lu, G. Y. Li, A. L. Swindlehurst, A. Ashikhmin, and R. Zhang, "An Overview of Massive MIMO: Benefits and Challenges," *IEEE Journal of Selected Topics in Signal Processing*, vol. 8, no. 5, pp. 742–758, Oct 2014.

[7] S. Salous, V. Degli Esposti, F. Fuschini, R. S. Thomae, R. Mueller, D. Dupleich, K. Haneda, J. Molina Garcia-Pardo, J. Pascual Garcia, D. P. Gaillot, S. Hur, and M. Nekovee, "Millimeter-Wave Propagation: Characterization and modeling toward fifth-generation systems. [wireless corner]," *IEEE Antennas and Propagation Magazine*, vol. 58, no. 6, pp. 115–127, Dec 2016.

[8] A. Richter, *Estimation of Radio Channel Parameters: Models and Algorithms*. ISLE, 2005. [Online]. Available: https://books.google.fr/books?id=XZEVMQAACAAJ

[9] F. Quitin, C. Oestges, F. Horlin, and P. De Doncker, "A Polarized Clustered Channel Model for Indoor Multiantenna Systems at 3.6 GHz," *IEEE Transactions on Vehicular Technology*, vol. 59, no. 8, pp. 3685–3693, Oct 2010.

[10] A. Bamba, M. Martinez-Ingles, D. P. Gaillot, E. Tanghe, B. Hanssens, J. Molina-Garcia-Pardo, M. Lienard, L. Martens, and W. Joseph, "Experimental Investigation of Electromagnetic Reverberation Characteristics as a Function of UWB Frequencies," *IEEE Antennas and Wireless Propagation Letters*, vol. 14, pp. 859–862, 2015.

[11] D. P. Gaillot, E. Tanghe, W. Joseph, P. Laly, V. Tran, M. Liénard, and L. Martens, "Polarization Properties of Specular and Dense Multipath Components in a Large Industrial Hall," *IEEE Transactions on Antennas and Propagation*, vol. 63, no. 7, pp. 3219–3228, July 2015.

[12] J. Poutanen, J. Salmi, K. Haneda, V. Kolmonen, and P. Vainikainen, "Angular and Shadowing Characteristics of Dense Multipath Components in Indoor Radio Channels," *IEEE Transactions on Antennas and Propagation*, vol. 59, no. 1, pp. 245–253, Jan 2011.

[13] K. Haneda, C. Gustafson, and S. Wyne, "60 GHz Spatial Radio Transmission: Multiplexing or Beamforming?" *IEEE Transactions on Antennas and Propagation*, vol. 61, no. 11, pp. 5735–5743, Nov 2013.

[14] K. Haneda, J. Järveläinen, A. Karttunen, M. Kyrö, and J. Putkonen, "A Statistical Spatio-Temporal Radio Channel Model for Large Indoor Environments at 60 and 70 GHz," *IEEE Transactions on Antennas and Propagation*, vol. 63, no. 6, pp. 2694–2704, June 2015.

[15] K. Saito, J. Takada, and M. Kim, "Dense Multipath Component Characteristics in 11-GHz-Band Indoor Environments," *IEEE Transactions on Antennas and Propagation*, vol. 65, no. 9, pp. 4780–4789, Sep. 2017.

[16] J. Pascual-Garcia, M. Martinez-Ingles, J. M. Garcia-Pardo, J. Rodriguez, and L. J. Lläcer, "Using tuned diffuse scattering parameters in ray tracing channel modeling," in *2015 9th European Conference on Antennas and Propagation (EuCAP)*, April 2015, pp. 1–4.

[17] J. Li, B. Ai, R. He, Q. Wang, B. Zhang, M. Yang, K. Guan, and Z. Zhong, "Directional analysis of indoor massive mimo channels at 6 ghz using sage," in *2017 IEEE 85th Vehicular Technology Conference (VTC Spring)*, June 2017, pp. 1–5.

[18] J. Li, B. Ai, R. He, M. Yang, and Z. Zhong, "On Modeling of Dense Multipath Component for Indoor Massive MIMO Channels," *IEEE Antennas and Wireless Propagation Letters*, vol. 18, no. 3, pp. 526–530, March 2019.

[19] F. Challita, M. Martinez-Ingles, M. Liénard, J. Molina-Garcia-Pardo, and D. P. Gaillot, "Line-Of-Sight Massive MIMO Channel Characteristics in an Indoor Scenario at 94 GHz," *IEEE Access*, pp. 1–1, 2018.

[20] K. Guan, G. Li, T. Kürner, A. F. Molisch, B. Peng, R. He, B. Hui, J. Kim, and Z. Zhong, "On Millimeter Wave and THz Mobile Radio Channel for Smart Rail Mobility," *IEEE Transactions on Vehicular Technology*, vol. 66, no. 7, pp. 5658–5674, July 2017.

[21] J. R. L. J.-L. J. P.-G. Vicent M. Rodrigo-Penarrocha, Lorenzo Rubio and J.-M. Molina-García-Pardo, "Millimeter wave channel measurements in an intra-wagon environment," *European Cooperation in Science and Technology EURO-COST Cartagena, Spain*, 2019.

[22] D. Hill, "Electromagnetic Fields in Cavities: Deterministic and Statistical Theories," *Antennas and Propagation Magazine, IEEE*, vol. 56, pp. 306–306, 02 2014.

[23] G. Steinböck, T. Pedersen, B. H. Fleury, W. Wang, and R. Raulefs, "Distance dependent model for the delay power spectrum of in-room radio channels," *IEEE Transactions on Antennas and Propagation*, vol. 61, no. 8, pp. 4327–4340, Aug 2013.

[24] S. Cheng, D. P. Gaillot, E. Tanghe, P. Laly, T. Demol, W. Joseph, L. Martens, and M. Liénard, "Polarimetric distance-dependent models for large hall scenarios," *IEEE Transactions on Antennas and Propagation*, vol. 64, no. 5, pp. 1907–1917, May 2016.